SCIENCE CHINA
Earth Sciences

Progress of Projects Supported by NSFC
• RESEARCH PAPER •

October 2013 Vol.56 No.10: 1629–1638
doi: 10.1007/s11430-013-4695-1

Cratering process and morphological features of the Xiuyan impact crater in Northeast China

WANG XinYuan[1,3], LUO Lei[1,2,3*], GUO HuaDong[1,3], MU LingLi[4], LI Chao[1,2,3], JI Wei[1] & CAI Heng[1,2,3]

[1] *Key Laboratory of Digital Earth Sciences, Institute of Remote Sensing and Digital Earth, Chinese Academy of Sciences, Beijing 100094, China;*
[2] *University of Chinese Academy of Sciences, Beijing 100049, China;*
[3] *International Centre on Space Technologies for Natural and Cultural Heritage under the Auspices of UNESCO, Beijing 100094, China;*
[4] *National Astronomical Observatories, Chinese Academy of Sciences, Beijing 100012, China*

Received April 21, 2013; accepted July 11, 2013; published online August 21, 2013

By using crater impact morphological theory and mathematics modeling, the paper studies the cratering process and morphological features of the Xiuyan Crater in Northeast China based on remote sensing imagery, digital elevation model (DEM) and drilling and measuring data. The results show that: 1) Simulated calculation indicates the diameter of the transient crater was 1406±12 m and the depth was 497±4 m. The diameter of the final crater was 1758±15 m and the depth was 374.5±3.5 m; the thickness of the breccia lens was 188.5±0.5 m. The data is basically the same as previous drilling data. 2) Preliminary determination of the size of Xiuyan impactor: The diameter at about 55 m for an iron meteorite, and about 115 m for a stony meteorite. 3) The depth-to-diameter ratio is 0.143, similar to the typical simple crater. The circularity index of the Xiuyan Crater is 0.884, indicating erosion and degradation. 4) The distribution pattern of radial fractures has priority in NW-SE and WNW-ESE and these fractures control the development and evolution of drainage inside the crater.

Xiuyan Crater, cratering process, size of impactor, crater rim, fracture

Citation: Wang X Y, Luo L, Guo H D, et al. Cratering process and morphological features of the Xiuyan impact crater in Northeast China. Science China: Earth Sciences, 2013, 56: 1629–1638, doi: 10.1007/s11430-013-4695-1

Impact craters are approximately circular concave structures on the surface of a planet, moon or other solid body in the solar system, formed by the hypervelocity impact of a smaller body with the surface, such as a large meteoroid, asteroid, comet or satellite. These impacts were important in the formation and evolution of the Earth, paleontology, rock-forming and the state of matter in the deep Earth [1–5]. The impact craters of the Earth can be divided into three morphologically distinct classes: simple, complex and impact basin, according to the petro-physical parameters of the target surface and the size, density and velocity of the impactor [6, 7]. So far, 179 terrestrial impact craters in 33 nations have been found on the Earth (http://www.unb.ca/passc/ImpactDatabase/index.html). Xiuyan Crater, the first confirmed meteorite impact crater in China [8, 9], was listed on the Earth Impact Database in 2010.

The mechanisms, structure and morphology of impact craters and their associated ejecta deposits on the Earth and planets have inspired numerous studies. Gault et al. [10] and Gault [11] developed the research of impact cratering mechanisms and structures; McGetchin et al. [12] and Schultz [13] focused on the thickness of ejecta deposits;

*Corresponding author (email: lluo@ceode.ac.cn)

© Science China Press and Springer-Verlag Berlin Heidelberg 2013

Shoemaker et al. [14] proposed geological studies of Meteor Crater, Arizona; pre-impact geological conditions, physical properties, energy calculations, meteorite and initial crater dimensions and orientations of joints, faults, and walls at Meteor Crater were symmetrically researched by Roddy [15]; Pike [16], Melosh [17] and Collins et al. [18] simulated cratering through mathematics modeling; Wang et al. [19] and Wang et al. [20] studied the morphology and geological structure of lunar craters based on images from the unmanned Chinese lunar orbiter Chang'e-1.

Chen et al. [9] in 2009 drilled a 307 m deep borehole at the centre of Xiuyan Crater. After penetrating 107 m of lacustrine sediments, a breccia lens of about 188 m in thickness was encountered. The crater-fill breccia consisted of deposits of rock clasts and fragments more or less shock-metamorphosed. The geological structure and stratigraphic configuration within the crater, shock-melted rocks and planar deformation features in quartz found in the basement rocks close to the crater rim and in the crater-fill breccia provide clear evidence for an impact origin of the Xiuyan Crater [9]. Studies of Xiuyan Crater presently concentrate on the tectonic geology, geochemistry and mineralogy [8, 9, 21–25], leaving a lack of research into the cratering process and morphology. Hence for this study mathematical modeling, remote sensing imagery, DEM and drilling and measuring data were all deployed to analyze crater morphology. The size of the impactor was estimated using the method proposed by Collins et al. [18] in 2005.

1 Overview of Xiuyan Crater and data

1.1 Xiuyan Crater

The Xiuyan Crater is located at 40°21′55″N, 123°27′34″E in the north of Liaodong Peninsula of Northeast China (Figure 1(a)). The crater is 16 km northeast of the county seat of Xiuyan Manchu Autonomous County, between the Mangniu and Shaozi rivers [9] (Figure 1(b)), both tributaries of the Dayang River in southeastern Liaoning province. It is a simple bowl-shaped crater located in a low mountain-hill region. Xiuyan Crater has a circular-cum-hexagonal shape with a rim-to-rim diameter of about 1800 m (Figure 1(c)). From rim top to crater bottom, the depth ranges between 135 and 230 m, averaging 150 m. The altitude of

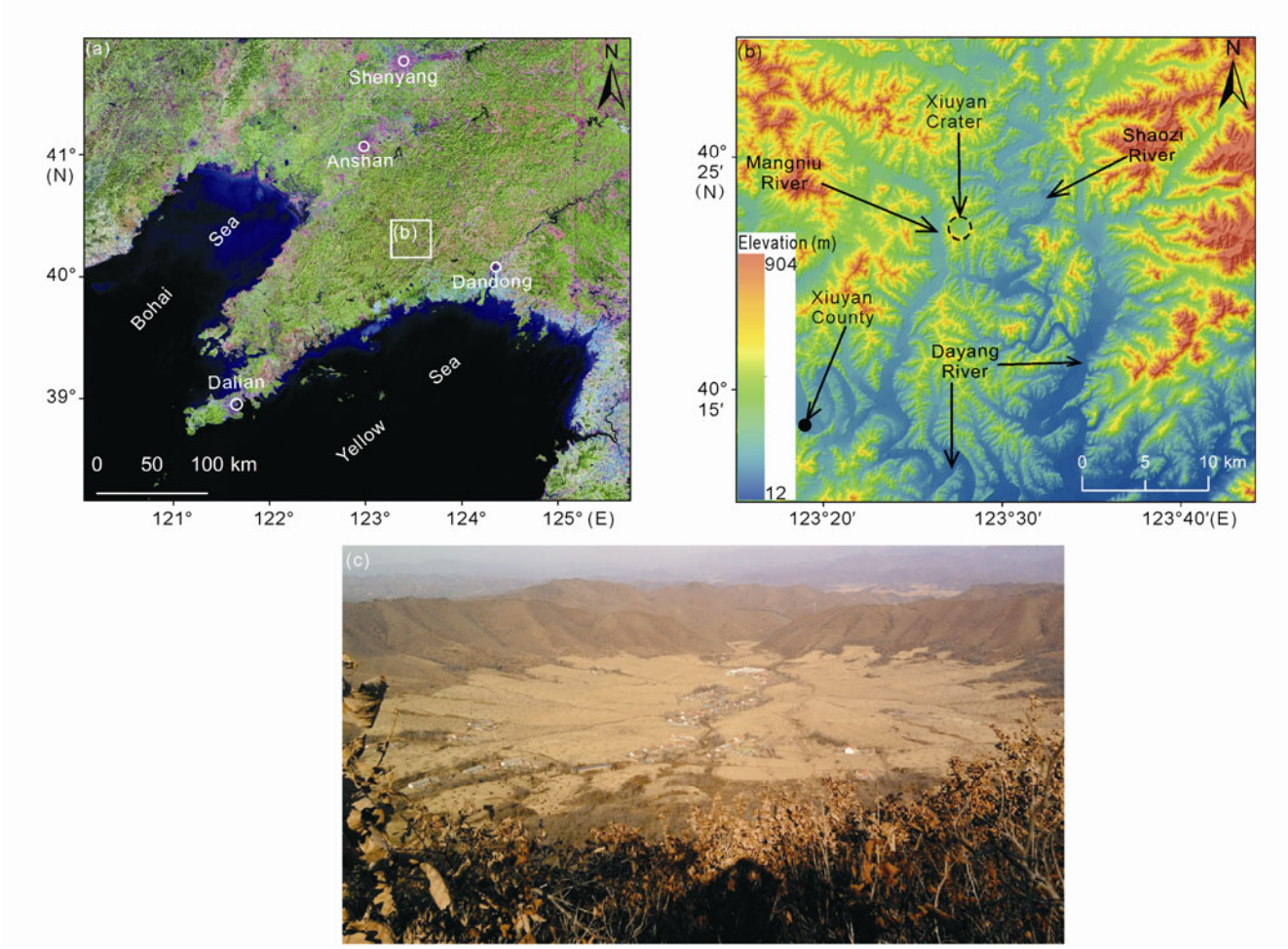

Figure 1 Xiuyan Crater. (a) Liaodong Peninsula by Landsat TM color composition (bands 7, 4, 2); (b) color shaded-relief map of Xiuyan Crater and surroundings (see inside white-box in (b) for location); (c) a panoramic view of Xiuyan Crater.

the central region on the floor of the crater is about 140 m [8, 9, 26].

Reasonably well-preserved, the Xiuyan Crater was created in the early Proterozoic (2 billion years ago) metamorphic rocks composed of leucoleptite, hornblendite, gneiss and marble [9, 27]. Both sides of the rim and the crest are covered with soil, eluvial and diluvial deposits a few meters thick. A few exposed basement rocks, mainly leucoleptite, stick out of the rim walls [8, 9]. Covered with Quaternary lacustrine sediments, the crater floor is used for farming and residential housing. The whole crater is coated with vegetation. Radial valleys emanate from inside the rims to meet at the crater center (Figure1(c)). These valleys generated gullies and a stream. The stream flows into the Shaozi River through a V-shaped gap in the northeast rim of the crater.

1.2 Data and preprocessing

In this paper, morphological parameters and cratering processes were calculated and developed by mathematics modeling, DEM, remote sensing data (Landsat ETM+ and Spot 5 image) and drilling and measuring data, and then the results were compared according to an analysis of the morphological features of the crater. We also analyzed geographical phenomena and features created by the meteorite impact.

DEM 2.5 meter-resolution data revealed the spatial distribution of topographic features in the study area (Figure 1(b)) using false color composite image after fusion of Spot 5's panchromatic band at 2.5-m spatial resolution and multispectral images at 10-m spatial resolution. Fieldwork conducted in November of 2011 included elevation, structure parameters and attitude of rock formation. For the Spot 5 image, a subdivision vector topographic map was used as a standard coordinate space to select the control points. Space geometry positions were transformed by collinearity equation and digital number (DN) values were resampled by cubic convolution.

2 Cratering inversion of Xiuyan Crater

2.1 Calculation of diameter and depth

In general, simple craters have smooth bowl-shape concave structures with a diameter of no more than 2000 m for sedimentary rock target type or 4000 m for crystalline rock target type [6, 7]. Simple craters have raised rims and overturned rim crests. Based on DEM, the highest $P1$ location of Xiuyan Crater is on the ridge of southwestern rim crest at 344 m; the lowest point $P2$ is in the northeast gap at 120 m (Figure 2). Fieldwork measured the same locations at 344.1 m and 120.3 m. DEM and fieldwork proved a good fit. The crater is approximately hexagonal (see white line in Figure 2) rather than pentagonal [8].

The DEM of the Xiuyan Crater and its surroundings, along with the radial direction through point C, in accordance with every 2° interval, are extracted profiles using 3D analysis in ESRI ARC-INFO V.10. Each profile curve P corresponds to a diameter of the Xiuyan Crater D_r. The average value of $D_r\left(=\frac{1}{90}\sum_{i=1}^{90}D_{r_i}\right)$ makes the Xiuyan Crater diameter 1804 m. By the same token, each profile curve P corresponds to two heights of the rim crest ridge H_r. The average value of H_r $\left(=\frac{1}{180}\sum_{i=1}^{180}(H_{r_i}-120)\right)$ finds the depth of the Xiuyan Crater to be 149 m.

The DEM extracted eight direction crater profiles, selected from the previous 90 profiles: N-S, NE-SW, E-W, NW-SE with average diameters of 1832, 1810, 1794, 1777 and 1803 m. The height of the rim crest ridge ranges from 220 to 344 m, with an average height of 269 m. The depth from ridge to crater bottom ranges from 100 to 224 m, averaging 149 m. Figure 3 and Table 1 show the extracted profiles and details.

2.2 Structural parameter inversion

The formation of an impact crater is an extremely complicated and dynamic process that can be divided into three stages: compression, excavation and modification [17]. One of the most important characteristics of meteorite impact is the deformation of target rocks, which produces an excavated cavity, uplifted rim and stratigraphically overturned ejecta blanket [17, 18]. The deformation occurs in a catastrophic burst of energy that fractures, melts and vaporizes material in a few seconds to a few minutes, depending on the size of the impact event. As a result, the target and impactor are rapidly compressed to very high pressures and heated to enormous temperatures. Between the compressed and uncompressed material, a shockwave is created that propagates away from point of impact. In the wake of the expanding shockwave, the target is comprehensively fractured, shock-heated, shaken and set in motion: leading to the excavation of transient craters many times larger than

Table 1 Structural parameters of Xiuyan Crater

Direction	Diameter (m)	Height of ridge (m)	Depth (m)
N	1832	260	140
S		280	160
NE	1810	N.A.[a)]	N.A.
SW		344	224
E	1794	260	140
W		240	120
NW	1777	280	160
SE		220	100
Average	1803	269	149

a) No available. The same below.

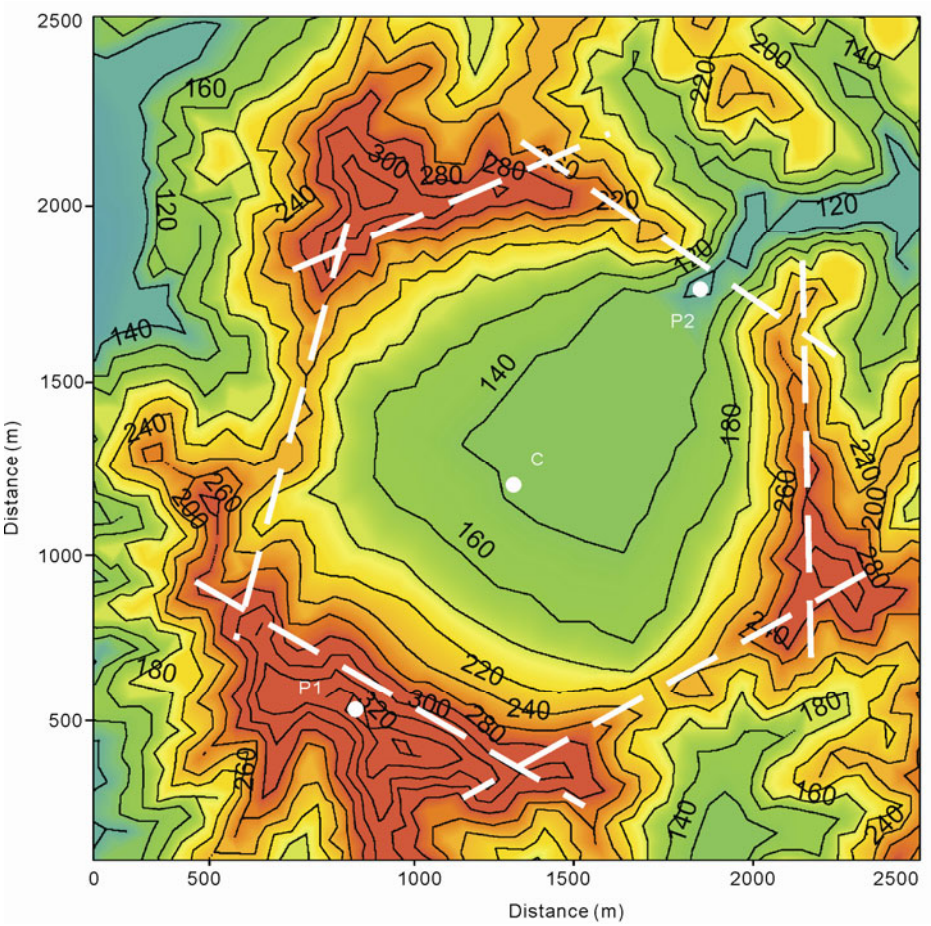

Figure 2 Map of the Xiuyan Crater showing location of borehole and sampling. Point C represents the drilling location in ref. [9].

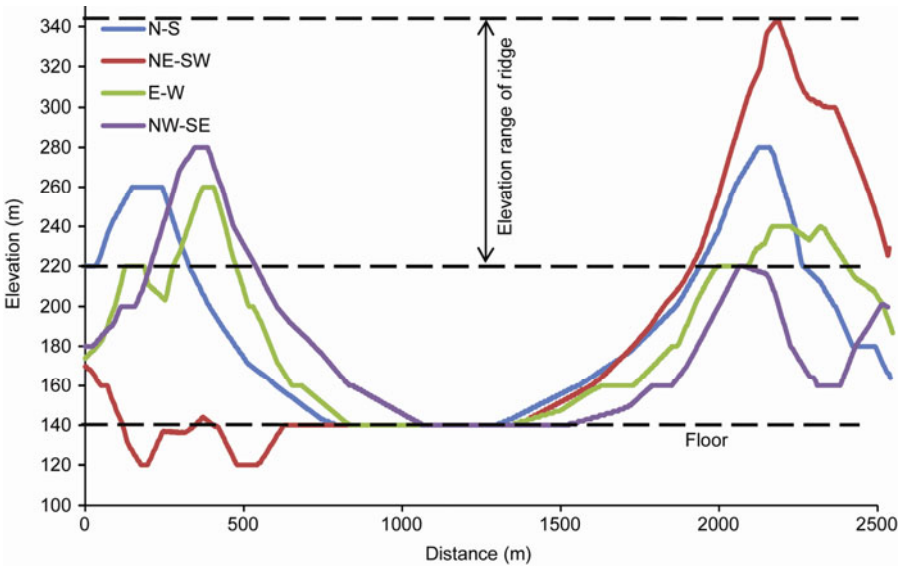

Figure 3 Profiles of Xiuyan Crater in eight directions.

the impactor itself [17]. This transient crater subsequently collapses under the influence of gravity to produce the final crater form. As the crater grows and collapses, fallback ejecta and debris slump in from the walls and rim to form crater-fill units or the breccia lens. Large volumes of rock debris are ejected onto the surface of the Earth surrounding

the crater. Close to the crater rim, this ejecta deposit forms a continuous blanket smothering the underlying terrain. The various dimensions of Xiuyan Crater, a bowel-shaped simple crater, are depicted and generalized in Figure 4.

D_{tr} is the diameter of the transient crater measured from rim crest to rim crest; D_{tc} is the transient crater diameter measured at the pre-impact surface; h_{tr} is the rim height of the transient crater measured from the pre-impact surface; d_{tc} is the depth of the transient crater measured from the pre-impact surface; D_{fr} is the diameter of the final crater measured from rim crest to rim crest; h_{fr} is the rim height above the pre-impact surface in the final crater; t_{br} is the breccia lens thickness; d_{fr} is the final crater depth measured from the crater floor (above the breccia lens) to the rim crest; t_e is the thickness of the ejecta deposits. We assume that the base of the breccia lens coincides with the floor of the transient crater at a depth of d_{tc} below the pre-impact surface; therefore, $d_{fr} = d_{tc} + h_{fr} - t_{br}$.

Simple craters are relatively small with depth-to-diameter ratios (d/D) of about 1∶5 to 1∶7 [16–18]. Previous morphological studies of simple craters [15–17, 28, 29] and the Earth impact effects program [18] have been validated in Meteor Crater, Arizona. The average depth of the well-preserved 1.2 km-diameter Meteor Crater is about 175 m [29], and the d/D value is about 0.146. In the Xiuyan Crater, as the breccia unit within the crater is covered by 107 m [9] of thick lacustrine sediments so the average depth around the top rim to above the breccia lens is about 295 m. The d/D value is about 0.143, similar to most simple impact craters. Collins' study can also be applied to the Xiuyan Crater based on this similarity. This study reconstructs the cratering process using measuring data. Collins et al. [18] proposed a mathematical model that simulates morphological and structural parameters for a simple crater:

$$D_{fr} \approx 1.25 D_{tc}, \tag{1}$$

$$D_{tr} = D_{tc}\sqrt{\frac{d_{tc} + h_{tr}}{d_{tc}}}, \tag{2}$$

$$d_{tc} = D_{tc} / (2\sqrt{2}), \tag{3}$$

$$d_{fr} = d_{tc} + h_{tr} - t_{br}, \tag{4}$$

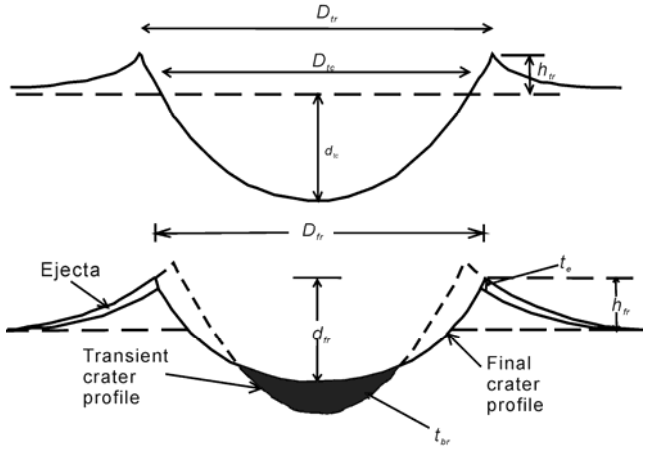

Figure 4 Cratering model of Xiuyan Crater (modified after refs. [17, 18]).

$$h_{fr} = 0.07\frac{D_{tc}^{\ 4}}{D_{fr}^{\ 3}}, \tag{5}$$

$$h_{tr} = D_{tc} / 14.1, \tag{6}$$

$$t_{br} = 2.8V_{br}\left(\frac{d_{tc} + h_{tr}}{d_{tc}D_{fr}^{\ 2}}\right), \tag{7}$$

$$V_{br} \approx 0.032 D_{fr}^{\ 3}, \tag{8}$$

$$t_e = \frac{h_{tr}}{8}\left(\frac{d_{tr}}{r}\right)^3, \tag{9}$$

where r is radial distance from the ejecta deposits to the center of crater. The simulation of morphological and structural parameters of Xiuyan transient crater and final initial crater are listed in Table 2. Here the D_{fr} is approximately equal to 1758±15 m; according to Roddy [15]: the diameter's ratio of present crater to final crater ranges from 1.017 to 1.035 based on Meteor Crater, Arizona.

According to Table 2 we know that the depth of the Xiuyan transient crater is about 497±4 m. Then the crater grew and collapsed, with fallback ejecta and debris slumping in from the walls and rim under the influence of gravity and rock mechanics [30]. This formed the breccia lens and lead to a final crater depth of about 374.5±3.5 m. In the

Table 2 Simulation results of morphological and structural parameters of Xiuyan Crater [a)]

	D_r (m)	D_c (m)	d_r (m)	d_c (m)	h_r (m)	t_{br} (m)	$t_e\|_{r=1000}$ (m)
Observation	1800	N.A.	150	N.A.	N.A.	188	0-4
Modification	1804	N.A.	256	N.A.	<50	N.A.	N.A.
Final	1758±15	1645±14	374.5±3.5	324±3	50.5±0.5	188.5±0.5	32±1
Transient	1540±13	1406±12	596.5±4.5	497±4	99.5±0.5	0	N.A.

a) Observation is based on refs. [8, 9]; the breccia unit within the crater is covered by 107 m thick lacustrine sediments. D_r is the diameter of the crater measured from rim to rim; D_c is the diameter of crater measured at the pre-impact surface; d_r is the crater depth measured from crater floor to rim; d_c is the crater depth measured from the crater floor to pre-impact surface; h_r is the rim height above the pre-impact surface, $t_e|_{r=1000}$ is the thickness of ejecta deposits at the r=1000 m.

Xiuyan Crater, the breccia lens has a simulated thickness of about 188.5±0.5 m, and this thickness is close to Chen's drilling result of 188 m [9]. The broad breccia lens suggests it has not eroded since formation. The bowl shape and thick bed of breccia within the crater demonstrate Xiuyan is well preserved.

2.3 Size estimation of impactor

Natural objects that encounter the Earth are either asteroids or comets and typically collide with the Earth's atmosphere at velocities of 12–20 km s^{-1} [28, 31]. The most likely impact angle is 45° [32]. Asteroids are made of iron (ρ_i = 8000 kg m^{-3}) or rock (ρ_i = 2000–3000 kg m^{-3}) [31, 33]. Detailed knowledge of the composition of comets is currently lacking; however, they are of much lower density (ρ_i = 500–1500 kg m^{-3}) and are composed mainly of ice [18]. For Xiuyan, we will consider an iron or rock asteroid impacting at 20 km s^{-1} into a sedimentary target (density = 2500 kg m^{-3}) [9, 27]. For the Xiuyan impact, we also assumed a standard impact angle of 45°.

Our simulation is based on the work of Collins et al. [18]. The equation relates the density of the target ρ_t and impactor ρ_i (in kg m^{-3}), the impactor diameter after atmospheric entry L (in meters), the impact velocity at the surface v_i (in m s^{-1}), the angle of impact θ (measured to the horizontal), and the Earth's surface gravity g_E (in m s^{-2}) to the diameter of the transient crater D_{tc} (in meters) as measured at the pre-impact target surface (Figure 5(a)):

$$D_{tc} = 1.161\left(\frac{\rho_i}{\rho_t}\frac{\rho_i}{\rho_t}\right)^{1/3} L_0^{0.78} V_0^{0.44} g_E^{-0.22} \sin^{1/3}\theta, \qquad (10)$$

where L_0 is the impactor diameter at the top of the atmosphere, V_0 is the velocity of the impactor at the top of the atmosphere, ρ_i is the impactor density, ρ_t is the target density, g_E is Earth's surface gravity at 10 m s^{-2}, and θ is the angle subtended between the impactor's trajectory and the tangent plane to the surface of the Earth at the impact point. Now we can estimate the size ranges of the Xiuyan impactor based on the inversion result of morphological and structural parameters and eq. (10).

Table 3 presents a comparison of the important parameters discussed in this paper for the Xiuyan impact event. The Xiuyan impact we consider are different sizes of iron (density = 8000 kg m^{-3}) or stony meteorite (density = 2700 kg m^{-3}) impacting at 20 km s^{-1} into a sedimentary target (density = 2500 kg m^{-3}).

(1) For a 50–55 m iron meteorite, the diameter of the final crater D_{fr} ranges from 1620 to 1810 m with an average diameter of 1715 m. The breccia lens t_{br} thickness ranges from 159 to 178 m, averaging 169 m.

(2) For a 55–60 m iron meteorite, the diameter of the final crater D_{fr} ranges from 1810 to 1990 m, with an average diameter of 1900 m. The breccia lens t_{br} thickness ranges from 178 to 196 m, averaging 187 m.

(3) For a 110–115 m stony meteorite, the diameter of the final crater D_{fr} ranges from 1650 to 1790 m, with an average diameter of 1720 m. The breccia lens t_{br} thickness ranges from 163 to 177 m, with an average thickness of 170 m.

(4) For a 115–120 m stony meteorite, the diameter of the final crater D_{fr} ranges from 1800 to 1920 m, with an average diameter of 1860 m. The breccia lens t_{br} thickness ranges from 177 to 190 m, with an average thickness of 184 m.

Details are listed in Table 3. Based on the diameter of the final crater and the thickness of breccias, a preliminary determination of the size of Xiuyan impactor is a diameter of about 55 m for iron and about 115 m for stony.

3 Rim profile/signature and fractures

3.1 Rim profile/signature

One of the most important impact features is deformation of target rocks including excavation, rim uplift and the ejecta deposits that consist of thrown-out debris derived from rock types exposed on the inner crater wall [34–36]. Erosion and sedimentation mask craters on Earth [6, 37]. A crater's morphological characteristics produce gradual change as time goes by, especially at the rim.

The highest DEM points all over the crater form the rim that acts as the rim profile/signature. Average rim heights in four directions are 280 m (north), 260 m (east), 320 m (south) and 220 m (west). From 344 m in the southwest down to 220 m in the west, the rim's unevenness is the result of erosion and degradation (Figure 5).

Table 3 Size of Xiuyan impactor

Parameters	Reference value	Calculation					
		Iron			Stony		
Size (m)	N.A.	50	55	60	110	115	120
Density (kg m^{-3})	N.A.	8000	8000	8000	2700	2700	2700
Velocity (km s^{-1})	N.A.	20	20	20	20	20	20
d_{fr} (m)	>256 a)	344	385	423	352	382	411
D_{fr} (m)	1758±15	1620	1810	1990	1650	1800	1920
t_{br} (m)	188 b)	159	178	196	163	177	190

a) Breccia unit within crater is covered by 107 m of thick lacustrine sediments; b) according to ref. [9].

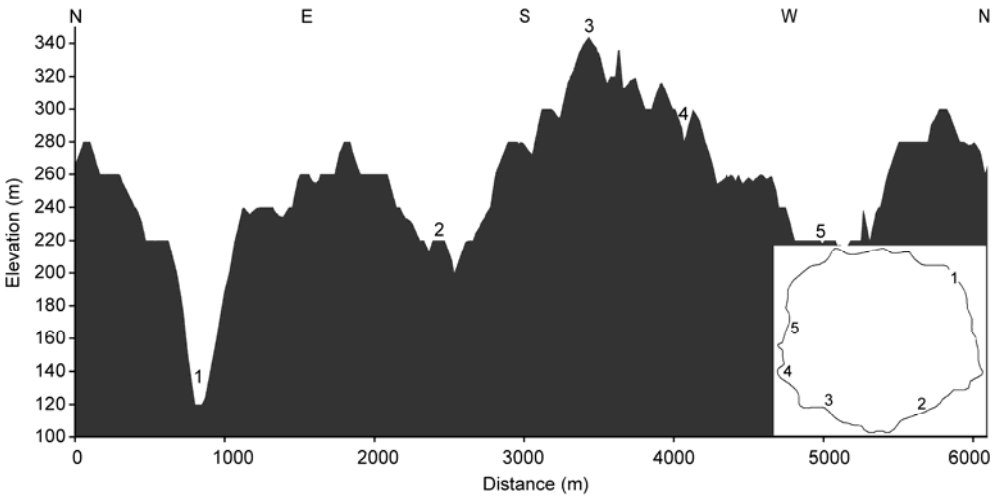

Figure 5 Rim signature of the Xiuyan Crater with features occurring on the rim. Location 1: The northeastern region shows erosion. Near-flat surfaces were observed more in the north. Location 2: The southeastern region has an opening in the rim, and this portion is also affected by erosion. Location 3: The southwestern region has the highest elevated point of 344 m. Location 4: This area hosts the best observed V-shaped protrusion caused by severe erosion. Location 5: A near-flat surface is observable in the western region.

Figure 6 shows the DEM extracted rim of Xiuyan Crater overlaid on Spot 5 image. The northeast part of the rim is severely eroded. As shown in Figure 6, the rim profile coincides well with the ridgelines. Circularity index (CI) is a measure of roundness: An impact crater's CI indicates its maturity, i.e. circularity decreases with age [38]. Xiuyan was calculated using $CI=4\pi\times area/perimeter^2$. Most research relies on two-dimensional images to compute CI. This study however utilized DEM and the extracted rim boundary to compute CI. It is appropriate to estimate the CI from elevation data rather than the 2D data. The CI for Xiuyan Crater is 0.884, which indicates it is less mature and near-circular in shape.

3.2 Structural fractures

A crater rim has three distinct groups of fractures: radial, concentric and conical. When the crater rim is restored to pre-impact condition, the radial and concentric fractures resemble pre-impact fracture populations, indicating that crater wall deformation and rim uplift were partly accommodated by activation of pre-existing fractures [35, 36]. Deformation of crater walls at Xiuyan Crater was accommodated in a series of radial, concentric and conical fractures. On the inside wall of the northern and eastern rims, there are radial valleys toward the centre of crater (Figure 1(c)). The radial valleys extend hundreds of meters from the top of rim to the floor of the crater. These radial valleys display broad arc outlines different from normally eroded ridges and valleys around this area, volcanic craters or any other landform [9].

Fractures are a kind of tectonic characteristic related to impact upon the bedrock of the crater wall. We drew fracture distribution maps of the crater wall (Figure 7(a)) using Spot 5 false color composite image with 2.5 m spatial resolution (Figure 6). Because of the geological process and complicated land cover of Xiuyan Crater, bedrock is not obvious and concentric fractures are hard to observe. Most fractures are radial. In general, the radial fractures have preferred orientations, in the direction of NW-SE and WNW-ESE, approximately parallel to the crater short walls (Figure 7(b)).

After the crater's formation, a special enclosed centripetal drainage system formed in the crater wall. Radial fractures controlled the whole drainage as shown in Figure 7(a). In this period, Xiuyan Crater was a lake basin. Through continuous fluvial erosion and transport, Quaternary lacustrine sediments were eventually formed [8, 9]. As time went by inside and outside forces including gravity, weathering and water affected the rim crest and both sides of the rim until they became mostly covered with weathering soil, eluvial and diluvial deposits up to several meters thick. Tussah shrubbery grows inside and outside the wall today. A gap formed at the northeast rim, leading to leakage from the lake. After that, the main targets for fluvial transformation were lacustrine sediments and slope deposits. Gullies and small rivers developed in the crater floor, becoming important drains. Through interaction with the outside environment, the entirely centripetal drainage opened into a semi-closed system (Figure 6).

4 Conclusion and discussion

China's first confirmed meteorite impact crater, Xiuyan Crater is basically a hexagonal/circular bowl. Based on the simple crater impact model, using remote sensing, DEM, drilling and field work data, this study analyzed the crater-

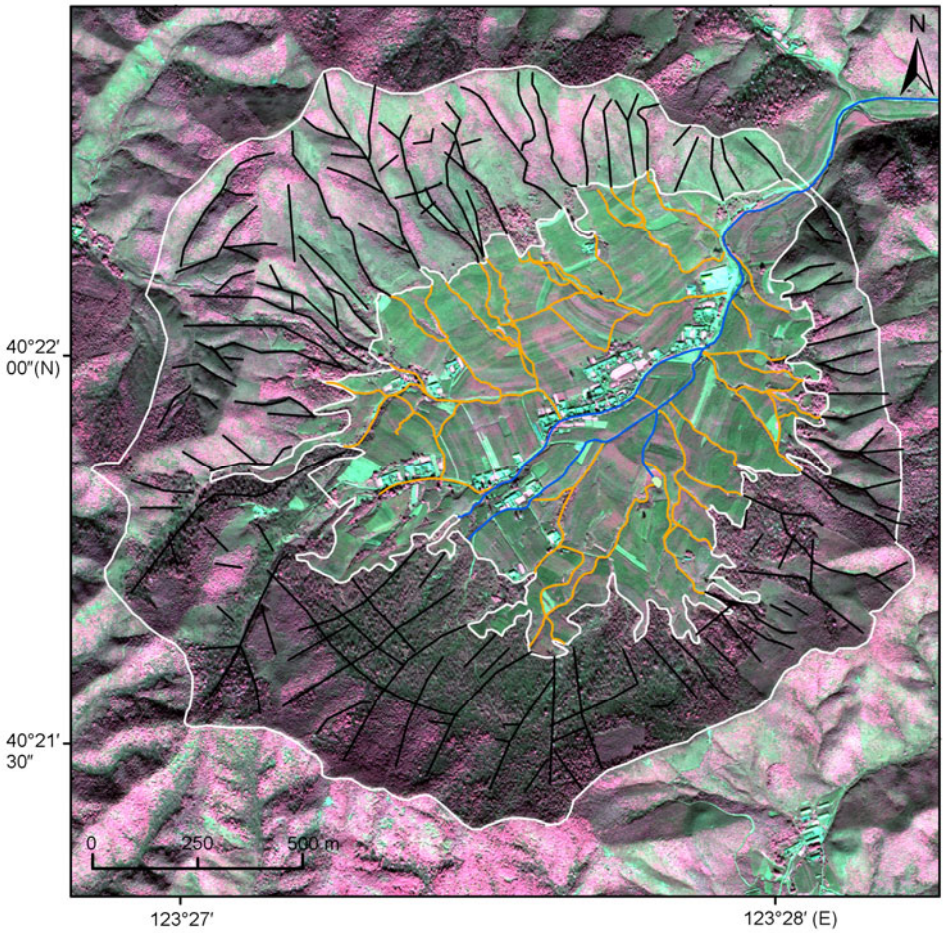

Figure 6 Spot 5 image and drainage system of Xiuyan Crater. White lines indicate inner and outer boundaries; black lines are crater wall fractures; yellow lines are gullies on the floor and blue are rivers.

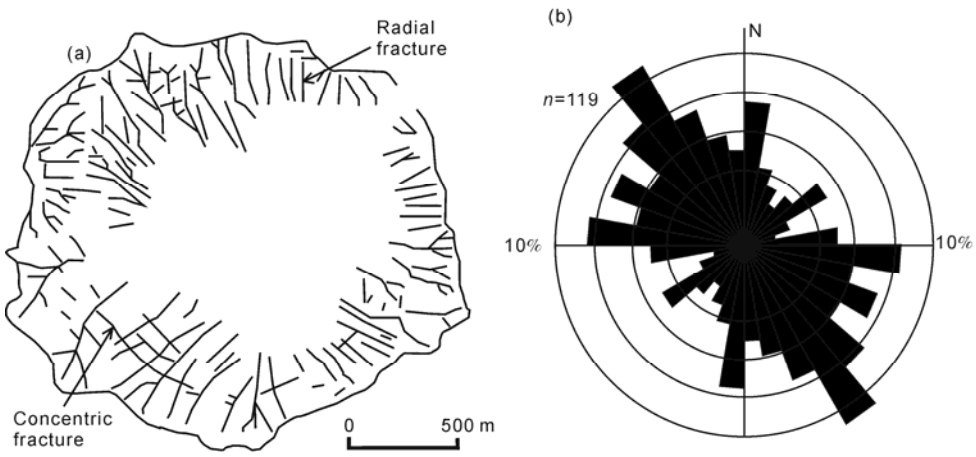

Figure 7 Impact fractures inside Xiuyan Crater. (a) Distribution map of impact fractures inside Xiuyan Crater based on interpretations of Spot 5 image; (b) directional rose diagram of the radial fractures representing all interpretations indicates preferential orientations.

ing process and morphological features: The diameter of the transient crater was 1406±12 m and the depth was 497±4 m. The diameter of the final crater was 1758±15 m and the depth was 374.5±3.5 m. The breccia lens has a simulated thickness of about 188.5±0.5 m, and this thickness is close to Chen's drilling result of 188 m. Preliminary determination of the size of the Xiuyan impactor indicates a diameter of about 55 m for iron meteorite and about 115 m for rock

meteorite. Therefore if the impactor which formed the Xiuyan Crater was not rock meteorite, the diameter must have been less than 100 m.

We also studied the morphological and structural features m of Xiuyan Crater based on DEM. The results showed a diameter of about 1804 m and a depth of about 149 m. The ratio of the distance between the crater rim crest and the top of breccia lens to the diameter of rim to rim is 0.143, the ratio of a typical simple meteor crater. The CI for Xiuyan Crater is 0.884, near-circular in shape and less mature. The profile/signature of the crater rim indicates erosion and degradation, especially the eroded gap in the northeast. The crater floor is covered with 107 m of Quaternary lacustrine sediment which demonstrates Xiuyan Crater used to be submerged and formed a closed lake.

Fracturing is one of the significant structural features related to the impact effect on bedrock of the crater wall. Fractures in the crater walls were interpreted via Spot 5 high-resolution false color composite imaging. The radial fractures have preferred orientations in NW-SE and WNW-ESE directions, approximately parallel to the crater short walls. This characteristic may be closely connected to the fracture distribution of the pre-impact surface. In addition, fractures in the walls are key control factors for the drainage system of the Xiuyan Crater. The initial enclosed centripetal drainage system opened up over time through interaction with the outside environment, indicating fluviation of the Xiuyan Crater.

We are grateful to researcher Hu Yuanman of Institute of Applied Ecology, Chinese Academy of Sciences, Professor Zhang Zhiquan of Shenyang University and Li Hong of Shenyang University for their kind help during fieldwork. Also appreciated was researcher Fu Bihong's assistance during paper writing and the technical assistance of Chang Chun from Institute of Remote Sensing and Digital Earth, Chinese Academy of Sciences. Many thanks are due to the reviewers for their constructive suggestions. This research was supported by National Natural Science Foundation of China (Grant No. 60972141), Strategic Priority Research Program of Chinese Academy of Sciences (Grant No. XDA04077200) and National High-Tech Research and Development Program of China (Grant No. 2010AA122202).

1 Covey C, Ghan S J, Walton J J, et al. Global environmental effects of impact-generated aerosols: Results from a general circulation model. In: Sharpton V S, Ward P D, eds. Global Catastrophes in Earth History. Boulder: Geological Society of America, 1990. 263–270
2 Toon O B, Zahnle K, Morrison D, et al. Environmental perturbations caused by the impacts of asteroids and comets. Rev Geophys, 1997, 35: 41–78
3 Kring D A. Impact events and their effect on the origin, evolution, and distribution of life. GSA Today, 2000, 10: 1–7
4 Ouyang Z Y. Small Astronomical Clashing and Ancient Environmental disaster: Research into Six Impact Events of the Cenozoic Era (in Chinese). Wuhan: Hubei Science and Technology Press, 1997
5 Fang J J, Wang J Q, Qiu X W, et al. Geoscience Significance and Identification of Meteorite Impact Structure (in Chinese). J Earth Sci Environ, 2008, 30: 234–239
6 Grieve R A, Shoemaker E M. The record of past impacts on Earth. In: Gehrels T, ed. Hazards Due to Comets and Asteroids. Tucson: University of Arizona Press, 1994. 417–462
7 Lin W Z. Research on impact craters with geophysical approaches (in Chinese). Geol-Geochem, 1998, 1: 63–68
8 Chen M. Impact-derived features of the Xiuyan meteorite crater. Chin Sci Bull, 2008, 53: 392–395
9 Chen M, Xiao W S, Xie X D, et al. Xiuyan Crater, China: Impact origin confirmed. Chin Sci Bull, 2010, 55: 1777–1781
10 Gault D E, Quaide W L, Oberbeck V R. Impact cratering mechanisms and structures, In: French B M, Short N M, eds. Shock Metamorphism of Natural Materials. Baltimore: Mono Book Corporation, 1968. 87–100
11 Gault D E. Impact cratering. In: Greeley R, Schultz P H, eds. A Primer in Lunar Geology. California: NASA Ames, Moffett Field. 1970. 137–175
12 McGetchin T R, Settle M, Head J W. Radial thickness variation in impact crater ejecta: Implications for lunar basin deposits. Earth Planet Sci Lett, 1973, 20: 226–236
13 Schultz P H. Atmospheric effects on ejecta emplacement. J Geophys Res, 1992, 97: 623–662
14 Shoemaker E M, Kieffer S W. Guidebook to the geology of Meteor crater, Arizona. Arizona: Arizona State University Press, 1974. 17–66
15 Roddy D J. Pre-impact geologic conditions, physical properties, energy calculations, meteorite and initial crater dimensions and orientations of joints, faults, and walls at Meteor crater, Arizona. The 9th Lunar Planetary Science Conference, 1978. 3891–3930
16 Pike R J. Control of crater morphology by gravity and target type: Mars, Earth, Moon. Houston. The 11th Lunar and Planetary Science Conference, 1980. 2159–2189
17 Melosh H J. Impact Cratering. New York: Oxford University Press, 1989. 245
18 Collins G S, Melosh H J, Marcua R A. Earth Impact Effects Program: A Web-based computer program for calculating the regional environmental consequences of a meteoroid impact on Earth. Met Planet Sci, 2005. 40: 817–840
19 Wang J, Zeng Z X, Yue Z Y, et al. Research of lunar tectonic features: Primary results from Chang'E-1 lunar CCD image (in Chinese). Chin J Space Sci, 2011, 31: 482–491
20 Wang X Y, Ji W, Li C, et al. Multi-parameters statistical analysis of impact craters' features on lunar surface based on Chang'e-1 (in Chinese). Geogr Res, 2012, 31: 369–376
21 Fan J C, Liu M J, Zhao C B, et al. Three-dimensional Q tomography for Xiuyan meteorite impact crater (in Chinese). Chin J Geophys, 2010, 53: 2367–2375
22 Chen M. Shock-metamorphic features of quartz in xiuyan crater (in Chinese). Acta Miner Sin, 2011, 2: 161–165
23 Zhao C B, Liu M J, Fan J C et al. High-resolution seismic exploration of Xiuyan impact crater structures (in Chinese). Chin J Geophys, 2011, 6: 1559–1565
24 Yi F, Chen M. Characteristics and genesis of siderite breccia from Xiuyan Crater (in Chinese). Geochimica, 2012, 6: 538–544
25 Chen M, Xiao W S, Xie X D, et al. The mineralogy evidence of the Xiuyan Crater (in Chinese). Acta Miner Sin, 2012, S1: 51
26 Zhao S M. Found an impact structure-crater in the Liaodong Peninsula Central Xiuyan Manchu Autonomous Region (in Chinese). Remote Sens Land Resour, 2004. 3: 27
27 Qin G J, Lu D R, Ou Q, et al. The discovery of PGE anomaly and platina from Luoquanli impact crater (in Chinese). Earth Sci Front, 2001, 8: 333–338
28 Grant J A. Evaluating the evolution of process specific degradation signatures around impact craters. Int J Impact Eng, 1999, 23: 331–340
29 Kring D A. Guidebook to the Geology of Barringer Meteorite Crater, Arizona. LPI Contribution No. 1355, 2007
30 French B M. Traces of Catastrophe: A Handbook of Shock-metamorphic Effects in Terrestrial Meteorites Impact Structure. Hou-

ston: Lunar and Planetary Institute, 1998. 23–29
31 Bottke W F J, Nolan M C, Greenberg R, et al. Collisional lifetimes and impact statistics of near-Earth asteroids. In: Gehrels T, ed. Hazards Due to Comets and Asteroids. Tucson: University of Arizona Press. 1994. 337–357.
32 Shoemaker E M. Interpretation of lunar craters. In: Kopal Z, ed. Physics and Astronomy of the Moon. New York: Academic Press, 1962. 283–359
33 Hilton J L. Asteroid masses and densities. In: Bottke W F J, Cellino A, Paolicchi P, et al., eds. Asteroids III. Tucson: University of Arizona Press, 2002. 103–112
34 Dence M R, Grieve R A F, Robertson P B. Terrestrial impact structures: Principal characteristics and energy considerations. In: Roddy D J, Pepin R O, Merrill R B, eds. Impact and Explosion Cratering. New York: Pergamon, 1977. 247–275
35 Kumar P S. Structural effects of meteorite impact on basalt: Evidence from Lonar Crater, India. J Geophys Res, 2005, 110(B12402): 1–10
36 Kumar P S, Kring D A. Impact fracturing and structural modification of sedimentary rocks at Meteor Crater, Arizona. J Geophys Res, 2008, 113(E09009): 1–17
37 Grieve R A. Impact bombardment and its role in proto-continental growth on the early earth. Precambrian Res, 1980, 10: 217–247
38 Adler J E M, Salisbury J W. Circularity of lunar craters. Icarus, 1969, 10: 37–52